Supplementary Material

Improving All Ternary Small-Molecule Organic Solar Cells by Optimizing Short Wavelength Photon Harvesting and Exciton Dissociation based on a Bisadduct analogue of [70]PCBM as a Third Component Materials

Zhiyong Liu[abc*] and Hong-En Wang[abc*]

[a]Institute of Physics and Electronic Information, Yunnan Normal University, Kunming 650500, China.

[b]Yunnan Key Laboratory of Optoelectronic Information Technology, Kunming 650500, China.

[c]Key Laboratory of Advanced Technique & Preparation for Renewable Energy Materials, Ministry of Education, Yunnan Normal University, Kunming 650500, China.

[*]Corresponding authors: (zhiyongliu1982@hotmail.com (Z.Y Liu); hongenwang@hotmail.com (H.E Wang))

Experimental section

Materials: BTR and Y6 were purchased from Solarmer Materials, Inc. Bis$PC_{71}BM$ and $PC_{71}BM$ was purchased from Luminescence Technology Co. *o*-Dichlorobenzene (ODCB) was purchased from Sigma-Aldrich Co. MoO_3 and Ag were purchased from Alfa Aesar Co. The BTR and the blend of Y6 and third component materials were dissolved in ODCB. The BTR:Y6 ratio was 1:1 (the total concentration was 20 mg mL^{-1}), and the bis$PC_{71}BM$ and $PC_{71}BM$ content was changed according to the measurement. The photoactive layer solution with the solvent additive of 1-chloronaphthalene (CN) (0.5%, v/v). The ZnO solution was synthesized by a sol-gel method [1, 2].

Device Fabrication: The ITO glass substrates (10 Ω per square) are clean via sequential sonication in detergent, deionized water and ethanol and then blow-dried with high-purity nitrogen. Subsequently, a ZnO solution was spin-coated on ITO substrates at 2000 rounds per min (RPM) for 40 s and dried at 150 °C for 2 min in atmospheric air. Then, ZnO/ITO substrates are transfer into a high-purity nitrogen-filled glove box. The photoactive solution was spin-coated onto the ZnO/ITO substrates at 1500 RPM for 40 s to prepare the photoactive layers, and thermally annealed at 120°C for 5 min. Finally, the MoO_3 layer and Ag electrode are deposit by thermal evaporation. The photoactive area, defined by the overlapping area of the ITO cathode and Ag anode, was approximately 9 mm^2 (3◊3 mm).

Device Measurement: AM 1.5G irradiation was provided by an XES-40S2 (SAN-EI ELECTRIC Co., Ltd) solar simulator (AAA grade, 5.0×5.0 cm^2 photobeam size) with a light intensity of 100 mW cm^{-2}. The current density-voltage (J-V) curves of all the OSCs were measured by a Keithley 2400 unit in a high-purity nitrogen-filled glove box. The absorption spectra of the films are measure with a Shimadzu UV-3101 PC spectrometer.

The R_S and R_{SH} are calculate according to the below expressions [3, 4]:

$$(\frac{dI}{dV})_{I=0} = \frac{1}{R_S}$$

$$(\frac{dI}{dV})_{V=0} = \frac{1}{R_{SH}}$$

The J-V curves under $I = 0$ and $V = 0$ are defined as the R_S and R_{SH} value. When $R_S = 0$ and $R_{SH} \rightarrow \infty$, which is corresponding to the $FF = 1$.

The crystallinity is related by Bragg's law [5, 6]:

$$\lambda = 2d\sin\theta$$

where λ is the wavelength of X-ray radiation (0.154 nm), θ is the peak position half angle and d is the inter-planer distance. The angles at which the peak intensities occur are related to the donor and acceptor molecule inter-planar distances of the thin films.

Table S1. The dependence of the V_{OC}, LUMO levels, energy bandgap and energy loss on the ratio of Y6:bisPC_{71}BM and Y6:PC_{71}BM.

Y6: bisPC_{71}BM	V_{OC} (V)	E_{LUMO} (eV)	E_{HOMO} (eV)	E_g (eV)	E_{loss} (eV)
1:0	0.860	-4.100	-5.650	1.240	0.380
1:0.1	0.888	-4.038	-5.639	1.302	0.414
1:0.15	0.899	-4.010	-5.634	1.330	0.430
1:0.2	0.916	-3.984	-5.629	1.356	0.440
1:0.25	0.923	-3.959	-5.625	1.381	0.458
1:0.3	0.938	-3.935	-5.621	1.405	0.467
0:1	1.040	-3.700	-5.460	1.640	0.600

Y6: $PC_{71}BM$	V_{OC} (V)	E_{LUMO} (eV)	E_{HOMO} (eV)	E_g (eV)	E_{loss} (eV)
1:0	0.860	-4.100	-5.650	1.240	0.380
1:0.1	0.870	-4.088	-5.660	1.252	0.382
1:0.15	0.880	-4.077	-5.664	1.263	0.383
1:0.2	0.888	-4.067	-5.669	1.273	0.385
1:0.25	0.895	-4.058	-5.673	1.282	0.387
1:0.3	0.901	-4.050	-5.677	1.290	0.389
0:1	0.940	-3.980	-5.870	1.360	0.420

Table S2. Summary of the molecular weight, *n*, *l*, and N_e values of Y6, bis$PC_{71}BM$ and $PC_{71}BM$.

Electron Acceptor	Molecular Weight (g mol^{-1})	*n* (mol g^{-1})	*l*	N_e (mol g^{-1})	E_{LUMO} (eV)
Y6	1451	4.15×10^{20}	1	4.15×10^{20}	-4.10
bis$PC_{71}BM$	887	6.79×10^{20}	1	6.79×10^{20}	-3.70
$PC_{71}BM$	680	8.85×10^{20}	1	8.85×10^{20}	-3.98

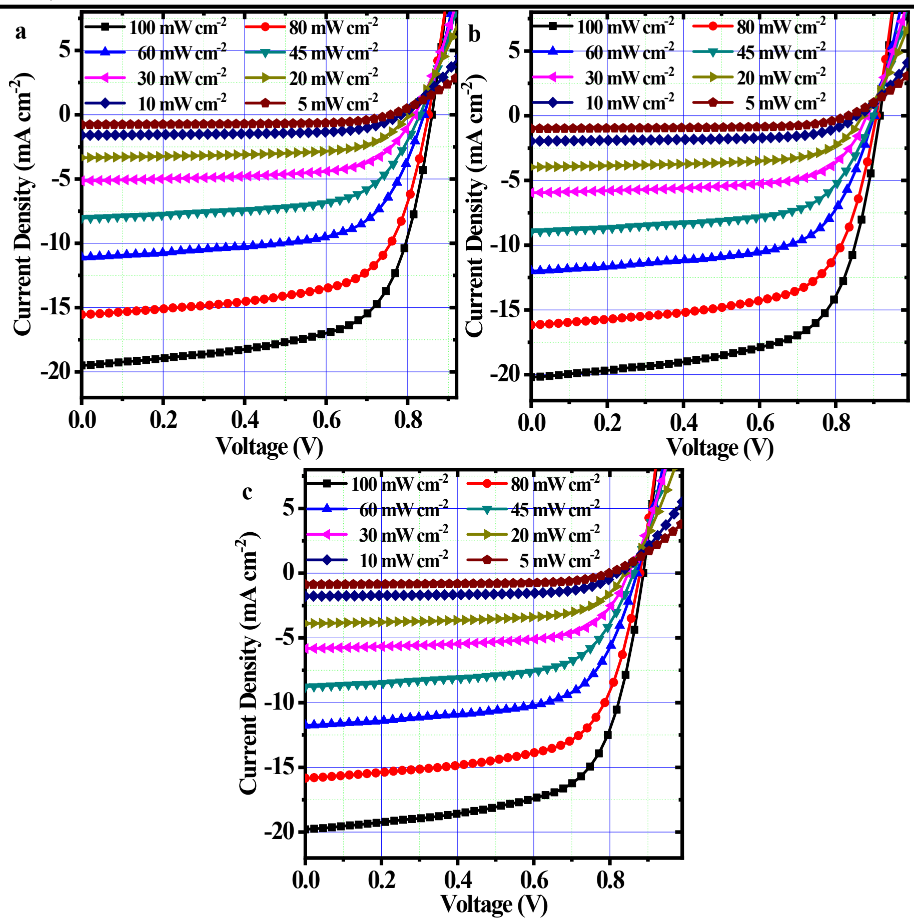

Figure S1. Dependence of the *J-V* characteristics on different light intensities (from

100 mW cm^{-2} to 5 mW cm^{-2}) for the BTR:Y6 binary PSCs, BTR:Y6:bisPC_{71}BM and BTR:Y6:PC_{71}BM-based optimized ternary PSC, corresponding to Figure S1(a), S1(b) and S1(c), respectively.

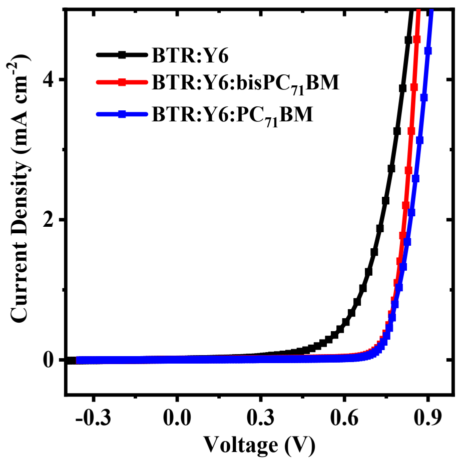

Figure S2. The dark current density of the BTR:Y6 binary PSCs, BTR:Y6:bisPC_{71}BM and BTR:Y6:PC_{71}BM optimized ternary PSCs.

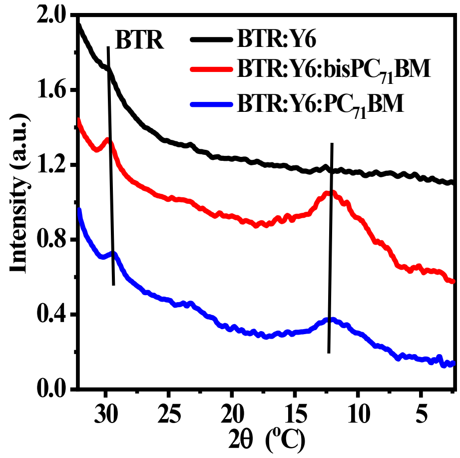

Figure S3. The XRD curves of the BTR:Y6 binary films, BTR:Y6:bisPC_{71}BM and BTR:Y6:PC_{71}BM optimized ternary film.

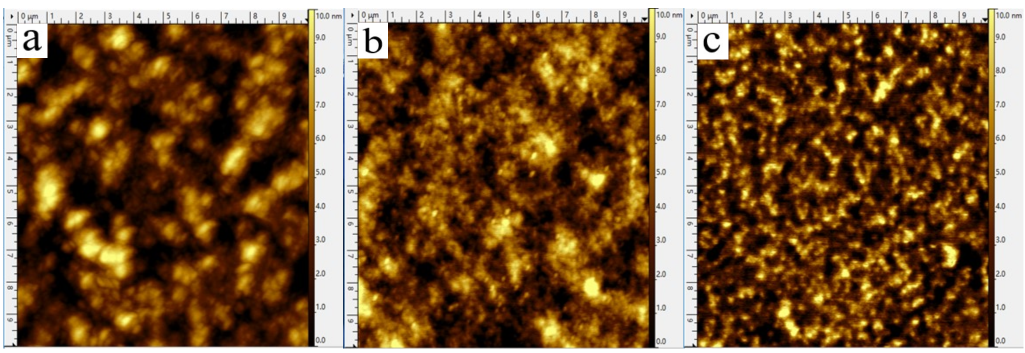

Figure S4. AFM images of the BTR:Y6 binary films, BTR:Y6:bisPC_{71}BM and BTR:Y6:PC_{71}BM optimized ternary film (a, b, c respectively).

Reference:

[1] W. Yu, L. Huang, D. Yang, P. Fu, L. Zhou, J. Zhang, C. Li, Efficiency exceeding 10% for inverted polymer solar cells with a ZnO/ionic liquid combined cathode interfacial layer, Journal of Materials Chemistry A, 3 (2015) 10660-10665.
[2] U. Galan, Y. Lin, G.J. Ehlert, H.A. Sodano, Effect of ZnO nanowire morphology on the interfacial strength of nanowire coated carbon fibers, Composites Science and Technology, 71 (2011) 946-954.
[3] F. Ghani, M. Duke, J. Carson, Numerical calculation of series and shunt resistances and diode quality factor of a photovoltaic cell using the Lambert W-function, Solar Energy, 91 (2013) 422-431.
[4] P.A. Chate, P.P. Hankare, D.J. Sathe, n-Type polycrystalline (CdZn)Se photoelectrode synthesis and its photoelectrochemical characterizations, Journal of Alloys and Compounds, 506 (2010) 673-677.
[5] A. Kulkarni, K.H. Schulz, T. Lim, M. Khan, Dependence of the sheet resistance of indium-tin-oxide thin films on grain size and grain orientation determined from X-ray diffraction techniques, Thin solid films, 345 (1999) 273-277.
[6] D. Zhao, W. Ke, C.R. Grice, A.J. Cimaroli, X. Tan, M. Yang, R.W. Collins, H. Zhang, K. Zhu, Y. Yan, Annealing-free efficient vacuum-deposited planar perovskite solar cells with evaporated fullerenes as electron-selective layers, Nano Energy, 19 (2016) 88-97.
[7] Y. Huo, X.-T. Gong, T.-K. Lau, T. Xiao, C. Yan, X. Lu, G. Lu, X. Zhan, H.-L. Zhang, Dual-Accepting-Unit Design of Donor Material for All-Small-Molecule Organic Solar Cells with Efficiency Approaching 11%, Chemistry of Materials, 30 (2018) 8661-8668.
[8] C. Xu, J. Wang, Q. An, X. Ma, Z. Hu, J. Gao, J. Zhang, F. Zhang, Ternary small molecules organic photovoltaics exhibiting 12.84% efficiency, Nano Energy, 66 (2019) 104119-104127.
[9] Z. Zhou, S. Xu, J. Song, Y. Jin, Q. Yue, Y. Qian, F. Liu, F. Zhang, X. Zhu, High-efficiency small-molecule ternary solar cells with a hierarchical morphology enabled by synergizing fullerene and non-fullerene acceptors, Nature Energy, 3 (2018) 952-959.
[10] Z. Liu, N. Wang, All small molecule ternary organic photovoltaic with two well compatible nonfullerene acceptors for minimizing energy loss, Solar Energy, 214 (2021) 110-118.
[11] Z. Liu, N. Wang, Efficient ternary all small molecule organic photovoltaics with NC70BA as third component materials, Dyes and Pigments, 187 (2021) 109111.
[12] D. Hu, Q. Yang, H. Chen, F. Wobben, V.M. Le Corre, R. Singh, T. Liu, R. Ma, H. Tang, L.J.A. Koster, T. Duan, H. Yan, Z. Kan, Z. Xiao, S. Lu, 15.34% Efficiency All-Small-Molecule Organic Solar Cells with Improved Fill Factor Enabled by A Fullerene Additive, Energy & Environmental Science, 13 (2020) 2134-2141.
[13] M. Jiang, H. Bai, H. Zhi, L. Yan, H.Y. Woo, L. Tong, J.-L. Wang, F. Zhang, Q. An, Rational compatibility in ternary matrix enables all-small-molecule organic solar cells with over 16% efficiency, Energy & Environmental Science, n/a (2021) n/a.